Band-Gap Dependence of the Ultrafast White-Light Continuum

A. Brodeur* and S. L. Chin

Centre d'Optique, Photonique et Laser and Département de Physique, Université Laval, Québec, Canada, G1K 7P4
(Received 17 September 1997)

We report an investigation of white-light continuum generation during self-focusing in extended transparent media using 140-fs Ti:sapphire laser pulses. A band-gap threshold is found above which the width of the continuum tends to increase with increasing band gap and below which there is no continuum generation. This is, to our knowledge, the first report of a parameter predicting the width of the continuum in condensed media. Multiphoton excitation of electrons into the conduction band is proposed as the primary mechanism reponsible for the observations. [S0031-9007(98)06156-0]

PACS numbers: 42.65.Re, 32.80.Rm, 42.65.Ky

A powerful ultrashort laser pulse focused into a transparent medium can be transformed into a white-light continuum ranging from the UV to the near IR [1–10]. This well-known phenomenon occurs in a wide variety of condensed media [1–6,9,10] and in gases [2,7,8]. Among the continuum's numerous applications we find time-resolved broadband absorption and excitation spectroscopy [2], optical pulse compression [2], optical parametric amplification [11], and characterization of laser-induced structural transitions [12].

Despite its widespread use, the white-light continuum remains far from being well understood. Particularly intriguing is the mechanism determining its spectral width. At present, it is generally accepted that the main mechanism in ultrafast continuum generation is strong self-phase modulation (SPM) enhanced by self-steepening of the pulse [6]. A shortcoming of this theory is its prediction of stronger SPM in media with higher Kerr nonlinearity, a trend that is not observed [2,9]. For instance, the continuum generated in water (a widely used medium) is among the broadest observed despite the low Kerr nonlinearity of water.

Self-focusing is believed to play a part in continuum generation in extended media. Indeed, it was found experimentally that the power threshold for continuum generation in gases coincides with the critical power for self-focusing [4,7,8]. This is not surprising, considering that the onset of catastrophic self-focusing at critical power leads to a drastic increase in intensity [13]. Self-focusing can also lead to the generation of free electrons, which contribute negatively to the index of refraction and can ultimately stop self-focusing by canceling the Kerr index [3,14]. The connection between continuum generation and self-focusing suggests that free electrons may be involved in continuum generation. Such a mechanism was first proposed by Bloembergen [3] to explain the picosecond continuum, in the form of SPM enhancement by avalanche ionization. With femtosecond pulses an important mechanism of free-electron generation in condensed media is multiphoton excitation (MPE) from the valence band to the conduction band, where electrons are essentially free [15].

This Letter provides new insight into continuum generation by femtosecond Ti:sapphire laser pulses in extended condensed media. Measurements with a new experimental technique confirm that continuum generation is triggered by self-focusing and reveal a strong dependence of the continuum on the band gap of the medium. A band-gap threshold is found below which the medium cannot generate a continuum and above which the width of the continuum increases with the band gap. This is, to our knowledge, the first report of a parameter predicting the width of the continuum in condensed media. We propose MPE as the primary mechanism responsible for the observations.

A Ti:sapphire laser system (Clark-MXR CPA-1) is used to generate 140-fs (FWHM) transform-limited pulses centered at $\lambda_0 = 796$ nm, with beam diameter 2.2 mm ($1/e^2$ of intensity). A new technique, shown in Fig. 1(a), is used to measure the evolution of the pulse spectrum, pulse energy, and beam profile during propagation [16]. The beam
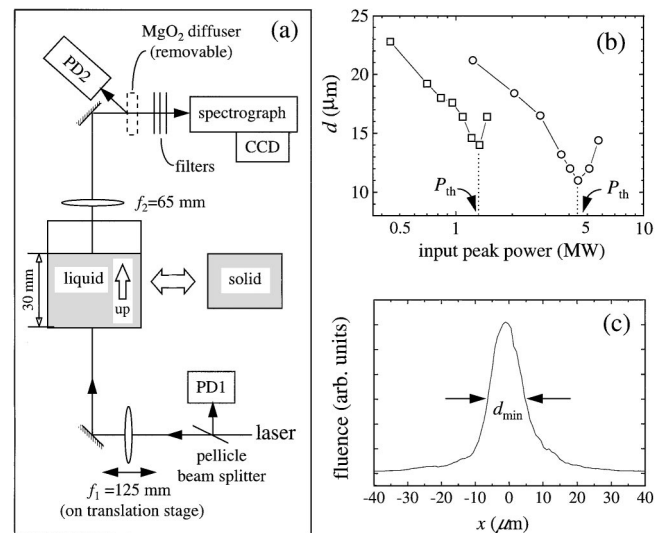

FIG. 1. (a) Experimental setup. (b) Beam diameter d (FWHM) at the geometrical focus, as a function of input peak power. Squares: C_2HCl_3 (trichloroethylene); circles: water. (c) Beam profile with diameter d_{min} at $P = P_{th}$ in water.

is focused with lens f_1 into the solid or liquid (contained in a stainless-steel cell equipped with two 3-mm fused-silica windows), where it propagates vertically upward. The input energy is measured with calibrated photodiode PD1 detecting the pellicle reflection. Only pulses within $\pm 1\%$ of the desired input energy are measured. The output spectrum and beam profile are measured by imaging with lens f_2 the output surface of the medium onto the entrance slit of the spectrograph (magnification 29.2×). To measure the pulse at various stages of propagation in the medium focusing lens f_1 is moved on a translation stage, such that the desired stage of propagation coincides with the output surface of the medium. Single-shot images are captured by a cryogenic 2D charge-coupled device (CCD) detector at the image plane of the spectrograph. The beam profile (spectrum) is measured by setting the spectrograph to zero (first) order. Filters are used to isolate different parts of the spectrum: BG18 for $\lambda < 630$ nm and RG850 for $\lambda > 850$ nm. The spectra are corrected for filter, grating, and CCD responses. The total transmitted pulse energy (hence energy loss) is measured with calibrated photodiode PD2 detecting light scattered by a (removable) MgO_2 diffuser and averaged over 50 shots. Energies are corrected for the photodiode's spectral response ($\sim 1\%$ overestimation in the worst case). The media listed in Table I are investigated.

Let us first consider the effect of self-focusing on the diameter d (FWHM) of the beam at the geometrical focus. This is measured by first positioning lens f_1 such that the geometrical focus is at the output surface of the medium and then varying the input power. At low power $d \simeq 27$ μm in all media. With increasing power d decreases, reaches a minimum d_{min} at the threshold power

TABLE I. Anti-Stokes broadening $\Delta\omega_+$ and self-focal characteristics measured at $P = 1.1P_{th}$: minimum beam diameter d_{min} (FWHM) (± 0.5 μm), maximum fluence F_{max} ($\pm 10\%$), and energy loss E_{loss} ($\pm 1\%$). P_{th} is accurate within $\pm 20\%$. E_{gap} is obtained from the medium's absorption spectrum, which generally exhibits a sharp absorption edge in the UV corresponding to E_{gap}.

Medium	E_{gap} (eV)	$\Delta\omega_+$ (cm^{-1})	d_{min} (μm)	F_{max} (J/cm^2)	E_{loss} (%)	P_{th} (MW)
LiF	11.8	19 800	10.8	1.3	13	8.8
CaF$_2$	10.2	18 300	10.4	1.0	11	7.4
Water	7.5	14 600	9.8	0.62	4	4.4
D$_2$O	7.5	14 600	10.6	0.46	4	3.6
Fused silica	7.5	13 500	10.4	0.57	3	4.3
Propanol	6.2	14 200	9.1	0.57	3	3.3
Methanol	6.2	14 500	10.2	0.54	4	3.9
NaCl	6.2	9000	9.9	0.29	3	2.0
1,4-Dioxane	6.0	10 200	9.3	0.44	3	2.7
Chloroform	5.2	11 200	10.0	0.29	1	2.2
CCl$_4$	4.8	10 400	8.7	0.44	2	2.5
C$_2$HCl$_3$	4.7	950	14.6	0.08	<1	1.2
Benzene	4.5	600	14.0	0.07	<1	0.90
CS$_2$	3.3	400	15.6	0.01	<1	0.23
SF-11 Glass	3.3	340	15.6	0.03	3	0.52

P_{th}, and then increases [see Fig. 1(b)] [17]. P_{th}, which is defined as the peak power at the entrance of the medium, corresponds to the critical power for self-focusing [13]. The beam profile with diameter d_{min} measured in water at input peak power $P = P_{th}$ is shown in Fig. 1(c). When the power is increased above P_{th} the position where d_{min} occurs moves closer to the entrance of the medium (~ 500 μm before the geometrical focus in all media when $P = 1.1P_{th}$). Above P_{th}, d_{min} remains practically constant. For instance, in water d_{min} remains within 0.5 of 10 μm from $P = 1.1P_{th}$ to $P = 2P_{th}$.

Self-focusing is accompanied in most media by white-light continuum generation. This occurs at $P \gtrsim P_{th}$, thus confirming that self-focusing triggers continuum generation. Examples of continua generated in water, NaCl, and LiF are shown in Fig. 2(a). Typical features are modulation near the laser wavelength and very strong Stokes/anti-Stokes asymmetry: the extent $\Delta\omega_+$ of the anti-Stokes pedestal reaches $\sim 10\,000-20\,000$ cm^{-1}, depending on the medium, while the extent $\Delta\omega_-$ of the Stokes pedestal is limited to a modest $\sim 1000-2000$ cm^{-1}. In some media there is no continuum generation; the spectra are comparatively much narrower and nearly symmetric. In all

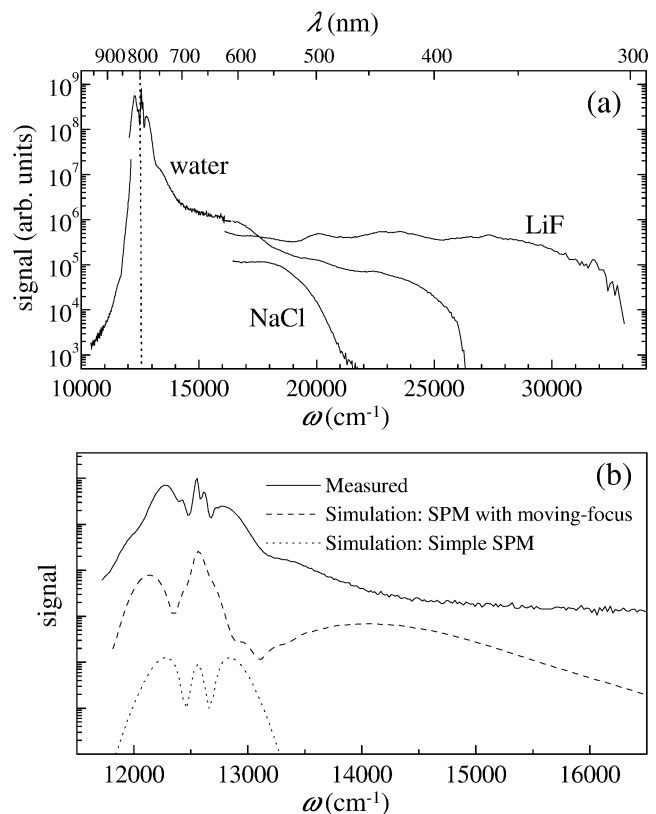FIG. 2. (a) White-light continuum spectrum generated in water, LiF, and NaCl at $P = 1.1P_{th}$. Only $\lambda < 630$ nm is shown for LiF and NaCl, for clarity. (b) Continuum spectra generated in water at $P = 1.1P_{th}$ in the experiment (solid line), in a 1D simulation including the moving-focus dynamics under MPE conditions (dashed line) and in simple SPM (dotted line). The simulations use $n_2 = 2 \times 10^{-16}$ cm^2/W, estimated from the measured P_{th}.

media there is usually an energy loss of a few percent at $P \gtrsim P_{th}$, occurring through the self-focus over a distance of typically 200–350 μm. The continuum develops concurrently with this energy loss.

The investigation revealed that continuum generation depends on the band gap E_{gap} of the material. The dependence of $\Delta\omega_+$ on E_{gap} at $P = 1.1P_{th}$ is shown in Fig. 3(a) and in Table I, along with various measured self-focal characteristics. The most striking observation is that continuum generation requires E_{gap} larger than the threshold value $E_{gap}^{th} \simeq 4.7$ eV. One can see in Table I that d_{min} also exhibits a discontinuity at E_{gap}^{th}. Typically, media with $E_{gap} < E_{gap}^{th}$ yield $d_{min} \sim 15$ μm, while media with $E_{gap} > E_{gap}^{th}$ yield $d_{min} \sim 10$ μm. Another surprising feature of the continuum is a trend of increasing $\Delta\omega_+$ with increasing E_{gap}. One can see that P_{th} also tends to increase with E_{gap}. This implies that $\Delta\omega_+$ increases with decreasing Kerr nonlinearity, since the critical power for self-focusing is inversely proportional to the Kerr index [13].

The observed continua cannot be explained by SPM theory alone: First, given the modest $\Delta\omega_-$ observed in all media, the SPM theory of Ref. [6] predicts $\Delta\omega_+ \simeq \Delta\omega_-$ (even when self-steepening is taken into account). This is clearly not the case; in water, for instance, we measure $\Delta\omega_+ \simeq 7\Delta\omega_-$. Second, the observation of increasing $\Delta\omega_+$ with decreasing Kerr nonlinearity is contrary to the prediction of SPM theory. In this light, it is clear that a complementary mechanism should be invoked. We will consider MPE, in view of the continuum's dependence on band gap.

The self-focal intensity achieved in water at $P = 1.1P_{th}$ is greater than 8×10^{12} W/cm^2 (estimated from the fluence and d_{min} measurements [17]). Recent studies

FIG. 3. (a) Anti-Stokes broadening $\Delta\omega_+$ vs band gap in various media. *a*, LiF; *b*, CaF$_2$; *c*, water; *d*, D$_2$O; *e*, UV-grade fused silica; *f*, 1-propanol; *g*, methanol; *h*, NaCl; *i*, 1,4-dioxane; *j*, chloroform; *k*, CCl$_4$; *l*, C$_2$HCl$_3$; *m*, benzene; *n*, CS$_2$; *o*, SF-11 glass. (b) Intensity required for MPE at rate $W = 10^{18}$ cm^{-3} fs^{-1} as a function of band gap (solid line). The curves for $W = 10^{17}$ cm^{-3} fs^{-1} and $W = 10^{19}$ cm^{-3} fs^{-1} are displayed for comparison. In both graphs the top axis shows the band gap normalized to the laser photon energy.

of laser-induced breakdown of water [18] have shown that a 100-fs pulse with a peak intensity of 5×10^{12} W/cm^2 can generate a free-electron density $N_e \simeq 10^{18}$ cm^{-3} mainly by MPE. In our experiment we estimate $1 \times 10^{17} < N_e < 1 \times 10^{19}$ cm^{-3}, based on the measured energy loss and self-focal dimensions. These values are consistent with $N_e^{stop} \simeq 10^{18}$ cm^{-3} required to stop self-focusing [3,14]. It is thus reasonable to assume that in this experiment self-focusing is stopped by MPE.

The ultrafast continuum can be explained by reviving Bloembergen's model of ionization-enhanced SPM [3,4] in the context of femtosecond pulses and MPE. During self-focusing a sharp intensity spike develops [3,13,19,20], which is limited by MPE up to a density $\sim N_e^{stop}$. Most of the MPE occurs at the very peak of the spike, during the half-cycle (1.3 fs) when the electric field is maximum (collisional ionization should be negligible in this short-duration spike and more important towards the back of the pulse). The appearance of free electrons by MPE during the intensity spike causes a sudden negative index change and thus a sudden drop in nonlinear phase. This translates into a large anti-Stokes broadening by SPM [3] (since the anti-Stokes broadening can be defined as $-(\partial\phi_{NL}/\partial\tau)_{min}$, where ϕ_{NL} is the nonlinear phase and τ is the time [13]).

This mechanism was simulated in a 1D calculation of propagation in water. The pulse is segmented into discrete temporal slices which self-focus independently according to the moving-focus model [13,19,20]. The total index change (a combination of the Kerr and free-electron indices) at a point in the medium where a slice self-focuses is assumed to have the following temporal distribution [21]: a slow increase during 100 fs, followed by a maximum lasting 10 fs and a drop to zero over 1.3 fs due to MPE. It is assumed that only slices in the leading half of the pulse suffer a significant index change, since self-focusing of the trailing half is attenuated by free electrons generated by the leading half [18,19]. The accumulated nonlinear phase throughout the pulse is obtained from the index changes associated with all the slices, and the resulting spectrum is computed by fast-Fourier transform. Setting the peak power to 1.1 times critical power and assuming a maximum intensity 1×10^{13} W/cm^2 yields the dashed-line spectrum in Fig. 2(b) (for comparison the corresponding simple-SPM spectrum is shown as a dotted line). The general shape of the dashed-line spectrum is similar to that of the measured spectrum, with a long but weak anti-Stokes wing. This simplified model thus reproduces the principal features of the observed spectrum. The main discrepancy is the anti-Stokes wing which falls off faster in the simulation than in the experiment. A better description would require more rigorous calculations, which are beyond the scope of the present Letter.

Now that we have established MPE-enhanced SPM as a plausible mechanism of continuum generation, let us see how it can explain the observed dependence of $\Delta\omega_+$
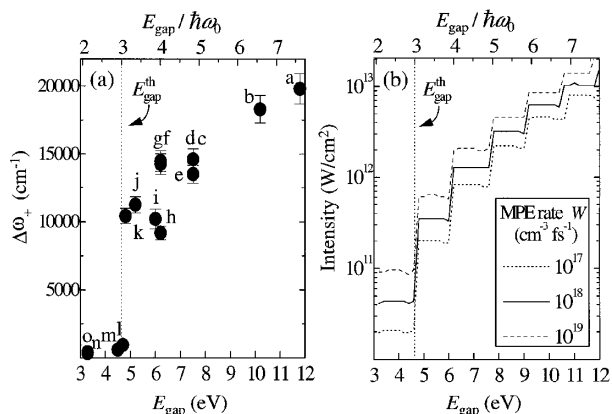
on E_{gap}. Generating $N_e^{stop} \simeq 10^{18}$ cm^{-3} during half an optical cycle requires a MPE rate $W \sim 10^{18}$ cm^{-3} fs^{-1}. The intensity I_{stop} yielding this rate can be calculated using the Keldysh theory of MPE in condensed media [15]. The results are shown in Fig. 3(b) as a function of E_{gap}. One can see a jump in I_{stop} at E_{gap}^{th}, due to passage from 3-photon to 4-photon MPE. Since E_{gap}^{th} is also the threshold for continuum generation, we can deduce that the intensity achieved in media with $E_{gap} > E_{gap}^{th}$ is sufficient to accumulate enough nonlinear phase for continuum generation. In media with $E_{gap} < E_{gap}^{th}$ self-focusing is stopped at lower intensities by free-electron defocusing (this agrees with the larger d_{min} observed in such media; see Table I). The increase of I_{stop} with E_{gap} is consistent with the observed trend of increasing $\Delta\omega_+$ with increasing E_{gap}: a higher I_{stop} implies a larger nonlinear phase and thus larger broadening. The fact that no clear discontinuities are observed in continuum behavior at $E_{gap} = 6.2$ eV, 7.8 eV, etc. could be due to the modification of the band structure in the presence of an intense field [22].

We note that group-velocity dispersion can play an important role in self-focusing of ultrashort pulses [20,23–26]. In particular, splitting of the pulse into two or more pulses [23,24,26] could occur prior to MPE. Finally, we remark that continua generated in gases [7,8] generally exhibit a weak dependence of $\Delta\omega_+$ on the medium (i.e., gas species) and a nearly symmetric spectrum, unlike the continua of this experiment. Continua from gases are also narrower ($\Delta\omega_+ \simeq 0.5\,\omega_0$) than those from condensed media ($\Delta\omega_+ \simeq 0.8\,\omega_0 - 1.6\,\omega_0$). The contribution of free electrons to continuum generation could therefore be more important in condensed media than in gases.

In conclusion, white-light continuum generation in transparent condensed media depends strongly on the medium's band gap. SPM enhancement by MPE (triggered by self-focusing) is a mechanism consistent with the observations. This sheds new light on continuum generation, attributed until now to strong SPM in a neutral medium.

---

    *Present address: National Research Council Canada, Industrial Materials Institute, 75 de Mortagne, Boucherville, Québec, Canada, J4B 6Y4.

[1] R. R. Alfano and S. L. Shapiro, Phys. Rev. Lett. **24**, 584 (1970).

[2] *The Supercontinuum Laser Source,* edited by R. R. Alfano (Springer-Verlag, New York, 1989).

[3] N. Bloembergen, Opt. Commun. **8**, 285 (1973).

[4] W. Lee Smith, P. Liu, and N. Bloembergen, Phys. Rev. A **15**, 2396 (1977).

[5] R. L. Fork, C. V. Shank, C. Hirlimann, R. Yen, and W. J. Tomlinson, Opt. Lett. **8**, 1 (1983).

[6] G. Y. Yang and Y. R. Shen, Opt. Lett. **9**, 510 (1984).

[7] P. B. Corkum, C. Rolland, and T. Srinivasan-Rao, Phys. Rev. Lett. **57**, 2268 (1986); P. B. Corkum and C. Rolland, IEEE J. Quantum Electron. **25**, 2634 (1989).

[8] F. A. Ilkov, L. Sh. Ilkova, and S. L. Chin, Opt. Lett. **18**, 681 (1993); V. François, F. A. Ilkov, and S. L. Chin, Opt. Commun. **99**, 241 (1993).

[9] G. S. He, G. C. Xu, Y. Cui, and P. N. Prasad, Appl. Opt. **32**, 4507 (1993).

[10] A. Brodeur, F. A. Ilkov, and S. L. Chin, Opt. Commun. **129**, 193 (1996).

[11] K. R. Wilson and V. V. Yakovlev, J. Opt. Soc. Am. B **14**, 444 (1997).

[12] E. N. Glezer, Y. Siegal, L. Huang, and E. Mazur, Phys. Rev. B **51**, 6959 (1995).

[13] J. H. Marburger, Prog. Quantum Electron. **4**, 35 (1975).

[14] E. Yablonovitch and N. Bloembergen, Phys. Rev. Lett. **29**, 907 (1972).

[15] L. V. Keldysh, Sov. JETP **20**, 1307 (1965).

[16] A. Brodeur and S. L. Chin, *QELS '97* [OSA Tech. Dig. Series **12**, 71 (1997)].

[17] d is the FWHM of the beam's fluence distribution (i.e., time-integrated distribution). d_{min} does not represent the smallest diameter achieved by a temporal segment of the pulse. The maximum intensity in the self-focus is thus larger than F_{max}/τ_0, where F_{max} is the maximum fluence and τ_0 is the pulse duration.

[18] Q. Feng, J. V. Moloney, A. C. Newell, E. M. Wright, K. Cook, P. K. Kennedy, D. X. Hammer, B. A. Rockwell, and C. R. Thompson, IEEE J. Quantum Electron. **33**, 127 (1997).

[19] A. Brodeur, O. G. Kosareva, C.-Y. Chien, F. A. Ilkov, V. P. Kandidov, and S. L. Chin, Opt. Lett. **22**, 304 (1997); O. G. Kosareva, V. P. Kandidov, A. Brodeur, C.-Y. Chien, and S. L. Chin, Opt. Lett. **22**, 1332 (1997).

[20] D. Strickland and P. B. Corkum, Proc. Soc. Photo-Opt. Instrum. Eng. **1413**, 54 (1991); D. Strickland and P. B. Corkum, J. Opt. Soc. Am. B **11**, 492 (1994).

[21] Y. R. Shen and M. M. T. Loy, Phys. Rev. A **3**, 2099 (1971).

[22] F. H. M. Faisal and R. Genieser, Phys. Lett. A **141**, 297 (1989).

[23] P. Chernev and V. Petrov, Opt. Lett. **17**, 172 (1992).

[24] J. Rothenberg, Opt. Lett. **17**, 583 (1992).

[25] G. G. Luther, J. V. Moloney, A. C. Newell, and E. M. Wright, Opt. Lett. **19**, 862 (1994).

[26] J. Ranka, R. W. Schirmer, and A. Gaeta, Phys. Rev. Lett. **77**, 3783 (1996).